Supplementary Material of Camera Trace Erasing

Chang Chen [1], Zhiwei Xiong ✉ [1], Xiaoming Liu [2], and Feng Wu[1]
[1] University of Science and Technology of China [2] Michigan State University
changc@mail.ustc.edu.cn, {zwxiong,fengwu}@ustc.edu.cn, liuxm@cse.msu.edu

1. Implementation Details of AD

We provide the implementation details of the gradient-based adversarial method (AD) [3]. As illustrated in Fig. 1(a), given an image im, AD requires a trained classifier $C(\cdot)$ and a known label lb, to generate the adversarial dithering ϵ from the back-propagation $C'(\cdot)$ of cross-entropy loss L_{ce}. The output im' is the summation between im and ϵ. Since the generation of ϵ requires a known label, AD cannot generalize to images with *unseen* camera types, as described in Section 4.3 of the main text. For more details, we adopt a ResNet trained on KCMI+ as the embodiment of $C(\cdot)$.

Moreover, for a full size image (with high resolution), AD should conduct the adversarial process patch by patch, as shown in Fig. 1(b), since $C(\cdot)$ usually has a size limit to its input (*e.g.*, 224×224 for the ResNet structure [4]). After adding the adversarial dithering, we gather the processed patches to obtain the full size output. Then, we randomly crop 4 patches from the full size output for evaluation, as described in Section 4.2 of the main text. We illustrate two of the randomly cropped patches im_* in Fig. 1(c) (colored in red) for a better understanding.

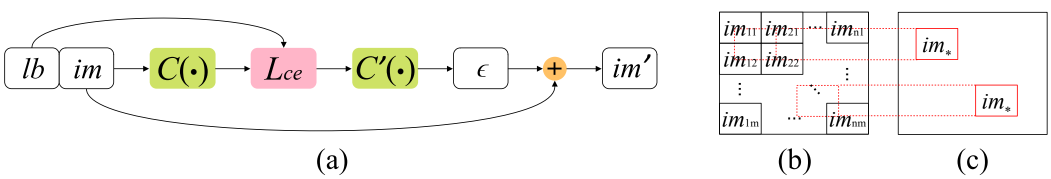

Figure 1. Implementation details of the gradient-based adversarial method [3] in the classification task.

2. Supplementary Visual Results

We provide supplementary visual results on KCMI-550 and VISION-1500.

As shown in Fig. 2, our proposed method has no visible destruction of content signal, such as the text on a yellow cab and the bright spots on a taillight. In comparison, MF, GF, and DN-E [2] blur the content signal in different degrees. While CP introduces the blocking artifact and degrades the visual quality.

As shown in Fig. 3, our proposed method effectively erases camera trace in the brown smooth area, without the visible destruction to the Roman numerals and patterns on a clock. In comparison, MF smooths out camera trace as well as a part of content signal. While DN-I [6] removes the visible noise, the residual camera trace in processed images is more than ours, which is demonstrated by the worse anti-forensic performance listed in the main text. As for DB [7], it has little response to the other part of camera trace except for the blocking artifact, which makes it difficult to handle the complex camera trace, as the brown smooth area shown in Fig. 3. Such a characteristic is also reflected by the small L_1 distance (*i.e.*, the degree of manipulation) listed in the main text.

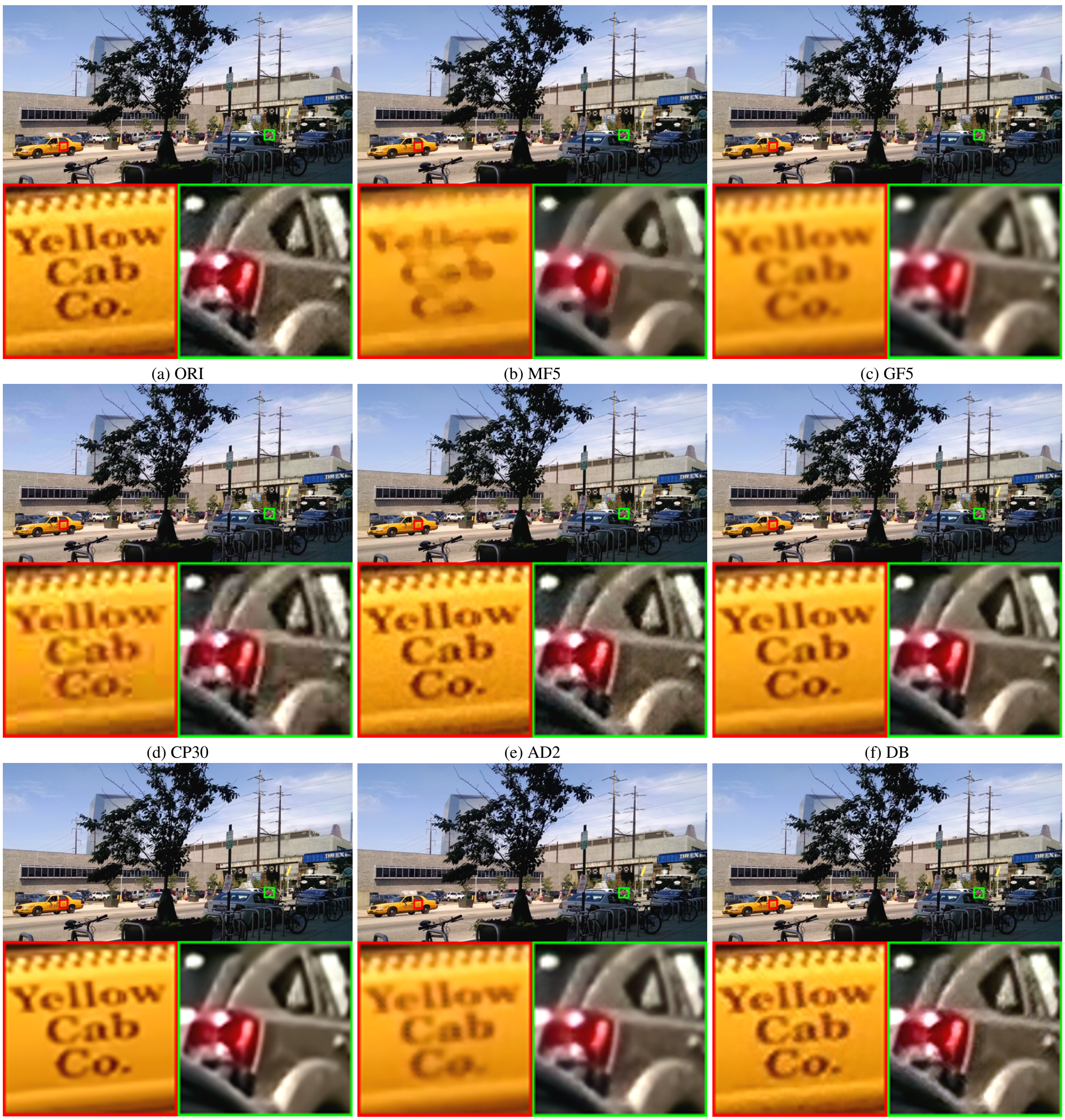

(a) ORI (b) MF5 (c) GF5

(d) CP30 (e) AD2 (f) DB

(g) DN-I (h) DN-E (i) Ours

Figure 2. Visual comparison on an image from KMCI-550.

(a) ORI (b) MF3 (c) MF5

(d) GF5 (e) CP30 (f) DB

(g) DN-I (h) DN-E (i) Ours

Figure 3. Visual comparison on an image from VISION-1500.

3. Camera Types and Thumbnails of Datasets

We list the camera types of KCMI [1] and VISION [5] in Tables 1 and 2, respectively. Thumbnail images are provided in Figs. 4 and 5.

Table 1. Definitions of serial numbers for camera types in KCMI

Number	1	2	3	4	5	6	7	8	9	10
Camera	HTC1	LG5X	MotoMax	MotoNex6	MotoX	GalaxyN3	GalaxyS4	SonyNex7	iPhone4S	iPhone6

Table 2. Camera (sensor) types in VISION

GT-I8190N	iPhone4S *	EVA-L09	LG-D290	iPhone5C	iPhone6 *	Lenovo P70A	GT-P5210	iPhone4	GT-I9300
D5503	GT-S7580	VNS-L31	Lumia640	Redmi Note3	iPad Mini	RIDGE 4G	OnePlus A3003	ASUS-Z	iPhone6P
iPhone5	SM-G900F	GT-I8190	GRA-L09	GT-I9195	NEM-L51	OnePlus A3000	SM-T555	G6-U10	iPad2

* These two camera types also exist in KCMI-550 (*i.e.*, No. 9 and 10).

Figure 4. A part of thumbnail images from VISION-1500.

Figure 5. A part of thumbnail images from KCMI-550.

References

[1] Camera model identification. https://www.kaggle.com/c/sp-society-camera-model-identification. 4

[2] Chang Chen, Zhiwei Xiong, Xinmei Tian, Zheng-Jun Zha, and Feng Wu. Real-world image denoising with deep boosting. *IEEE Transactions on Pattern Analysis & Machine Intelligence*, 2019. 1

[3] Ian J Goodfellow, Jonathon Shlens, and Christian Szegedy. Explaining and harnessing adversarial examples. In *ICLR*, 2015. 1

[4] Kaiming He, Xiangyu Zhang, Shaoqing Ren, and Jian Sun. Deep residual learning for image recognition. In *CVPR*, pages 770–778, 2016. 1

[5] Dasara Shullani, Marco Fontani, Massimo Iuliani, Omar Al Shaya, and Alessandro Piva. Vision: a video and image dataset for source identification. *EURASIP Journal on Information Security*, 2017(1):15, 2017. 4

[6] Jun Xu, Lei Zhang, and David Zhang. A trilateral weighted sparse coding scheme for real-world image denoising. In *ECCV*, 2018. 1

[7] Kai Zhang, Wangmeng Zuo, Yunjin Chen, Deyu Meng, and Lei Zhang. Beyond a gaussian denoiser: Residual learning of deep cnn for image denoising. *IEEE Transactions on Image Processing*, 26(7):3142–3155, 2017. 1